

# Comparing particulate morphology generated from human-made cellulosic fuels to natural vegetative fuels

Sayaka Suzuki<sup>A</sup> and Samuel L. Manzello<sup>B,\*</sup>

For full list of author affiliations and declarations see end of paper

**\*Correspondence to:**

Samuel L. Manzello  
Reax Engineering, Berkeley, CA, USA  
Email: [manzello@reaxengineering.com](mailto:manzello@reaxengineering.com)

## ABSTRACT

**Background.** In wildland–urban interface (WUI) fires, particulates from the combustion of both natural vegetative fuels and engineered cellulosic fuels may have deleterious effects on the environment. **Aims.** The research was conducted to investigate the morphology of the particulate samples generated from the combustion of oriented strand board (OSB). Findings were compared to the particulate samples collected from the combustion of noble-fir branches. **Methods.** The exposure conditions were varied to induce either smouldering combustion or flaming combustion of the specimens. Particulate samples were collected using thermophoretic sampling. Scanning electron microscopy (SEM) and subsequent image analysis were used to characterise particle sizes. **Key results.** The morphology of the generated particulates was influenced by the state of combustion for OSB as well as noble-fir branches. **Conclusions.** The combustion state resulted in differences in the particulate morphology for both OSB and noble-fir branches. More than 85% of the analysed particle diameters were less than 1000 nm in size collected from OSB specimens during smouldering combustion. **Implications.** The findings are the first step to better quantifying the morphology of particulates generated during WUI fire outbreaks. The experimental protocols and analysis methods presented may shed light on a problem that impacts human health in the WUI.

**Keywords:** climate, combustion, human health, oriented strand board (OSB), particulates, scanning electron microscope (SEM), smouldering, thermophoretic sampling, wildland–urban interface (WUI).

## Introduction

Large outdoor fires continue to take lives and destroy infrastructure. Over nearly every continent, wildland fires that spread into cities or urban areas, known as wildland–urban interface (WUI) fires, have yielded massive damage (Chas-Amil *et al.* 2013; Bento-Gonçalves and Vieira 2020). The 2020 WUI fire season in the USA was unprecedented. Some recent WUI fires have occurred in South Africa, as well as the Marshal Fire in Colorado in December 2021.

Highly populated urban areas have been the scene of large urban fires. In Asia, city or urban fires have occurred for decades upon decades. The growth of informal settlements common in Southeast Asia/Africa has yielded significant damage. Informal settlements are unplanned settlements or areas where housing is not in compliance with current planning and building regulations (unauthorised housing).

The fire spread processes are indeed similar among informal settlement fires, urban or city fires, and WUI fires. Once the wildland fire encroaches upon a city or urban location, the fire spread processes will occur by identical physical processes to those in informal settlement fires and urban fires. These processes are shown in Fig. 1, from Suzuki and Manzello (2021).

Particulate and gaseous emissions from large outdoor fires are an important factor regarding health effects for society (Reisen *et al.* 2015). A consequence of large outdoor fires is the production of combustion products. These combustion products are known to cause extreme visibility issues and worries about health. Globally, the combustion of vegetative

**Received:** 16 June 2022

**Accepted:** 18 September 2022

**Published:** 11 October 2022

**Cite this:**

Suzuki S and Manzello SL (2023)  
*International Journal of Wildland Fire*  
32(1), 78–85. doi:[10.1071/WF22093](https://doi.org/10.1071/WF22093)

© 2023 The Author(s) (or their employer(s)). Published by CSIRO Publishing on behalf of IAWF. This is an open access article distributed under the Creative Commons Attribution-NonCommercial 4.0 International License (CC BY-NC)

OPEN ACCESS

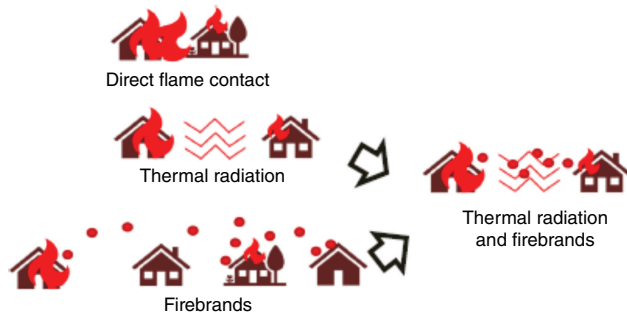


**Fig. 1.** Ignition mechanisms in large outdoor fires (Suzuki and Manzello 2021).

fuels is thought to be the prime supplier of particulate emissions and the second most supplier of gaseous emissions (Akagi *et al.* 2011). Particulate emissions from WUI fires in California in 2018 resulted in almost a complete closure of San Francisco. The production of particulates is known to influence the health of vegetation as well (Hemes *et al.* 2020).

Methodologies to determine emissions from wildland fires or biomass have centred on the concept of developing a specific emission factor (EF) (Akagi *et al.* 2011). EFs are usually reported for carbon monoxide, carbon dioxide, and particulate matter less than 2.5 microns. In many cases, EF does not account for the combustion of human-made fuels. It is obvious the vegetation species are not solely supplying the gaseous and particulate emissions but also the combustion processes from buildings, cars, buses, and other human-made combustibles only add to the assortment of emissions. Yet, it is not obvious how to address these additional complications.

Another overlooked shortcoming is that many of the EFs for vegetative fuels are predicated on controlled/prescribed fires. Specifically, these are well-controlled fires conducted for a variety of fire/fuel management intentions. Such controlled burning has benefits since it is performed over real terrain, but the fire exposure conditions cannot possibly recreate what is observed in the most dangerous fires. Typically, controlled fires are undertaken, under low ambient wind conditions to ensure safety yet massive, destructive fires rarely occur in low winds.

Complimenting EF research, there have been studies that have looked at the particulates formed in the context of wildland fires and as well as from biomass (Pósfai *et al.* 2003; Reid *et al.* 2005; Akagi *et al.* 2011). None of this important research has been extended to WUI fires, where many non-vegetative fuels exist. What has been observed is that the nature of particles formed depend highly on the nature of the smouldering or flaming combustion properties of the wildland fires or biomass.

The reasons for this lie in the details of the combustion processes. In the case of smouldering combustion, and therefore smouldering fires, this is a surface process. Oxygen moves to the surface and reacts with fuels at relatively low temperatures. Since polycyclic aromatic hydrocarbons (PAH)

are known to form at higher temperatures, smoke particles contain less soot for smouldering combustion as compared to flaming combustion. Particle formation is also known to occur around other nuclei other than PAHs (Dobbins and Megaridis 1987; Lighty *et al.* 2000; Dobbins 2007; Wang 2011; Michelsen 2017). For any type of large outdoor fire, there have been few studies of particulate formation in the smouldering phase and to the authors' knowledge, almost no studies for engineered wood products found in WUI fires (Hu *et al.* 2018).

Results reported that for wildland fires or biomass that are in a state of smouldering combustion, the combustion processes are generally dominated by lower temperature regimes and therefore the collected particles have a liquid-like structure (Pósfai *et al.* 2003; Reid *et al.* 2005; Akagi *et al.* 2011). For wildland fires or biomass that have higher temperatures, and are in a state of flaming combustion, these fires produce particles with more well-known fractal agglomerates and structures often seen in most soot formation studies in a state of flaming combustion.

Improved knowledge of large outdoor fire particulate emissions is needed at the laboratory scale. Here, samples of oriented strand board (OSB), a common human-made fuel abundant cities, were ignited using a radiant heater coupled to a spark igniter. Particulate samples were taken to begin to look at the morphology of the generated particulates. Using a simple experimental setup affords the capability to investigate particulates produced from smouldering combustion as well as those collected from flaming combustion.

As the nature of particulate samples was expected to be sensitive to the voltage of the electron beam for smouldering combustion in particular, scanning electron microscopy (SEM) was used as the first step to investigate the morphology. Transmission electron microscopy (TEM) operates at higher acceleration voltages and this is expected to influence the samples. Yet, TEM analysis, and in particular high-resolution TEM (HRTEM) is needed to provide finer details of the interior structures of the particulates (Das Chowdhury *et al.* 1996; Dobbins 1997; Chen and Dobbins 2000; Grieco *et al.* 2000; Hebgen *et al.* 2000; Vander Wal and Tomasek 2003; Shaddix *et al.* 2005).

## Experimental description

All work was completed at experimental facilities at the National Research Institute of Fire and Disaster (NRIFD). The experimental setup consisted of a radiant heater coupled to a spark igniter (see Figs 2, 3). Samples of OSB were cut into sizes of 100 mm × 100 mm. As commercial samples of OSB were used, the thickness was fixed at 11 mm.

The use of engineered wood products has been common worldwide. In the USA, there has been a move to replace the plywood with OSB. In the past, plywood was more common (White and Winandy 2006). OSB is manufactured from smaller trees and is manufactured primarily of wood fragments,

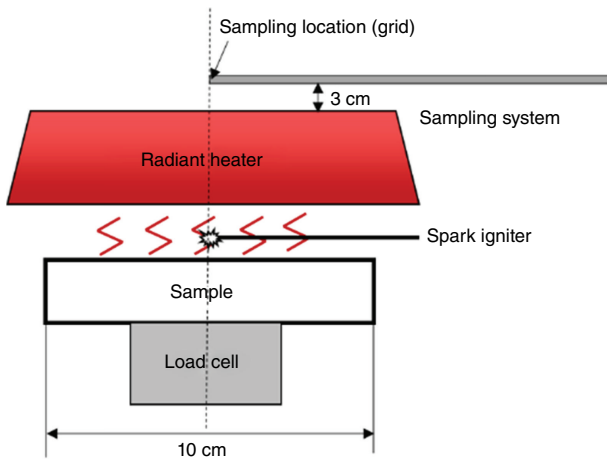


**Fig. 2.** Radiant heat source ignition source (side view).

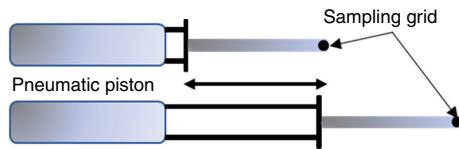


**Fig. 3.** Particle sampling system (side view).



**Fig. 4.** OSB sample is shown on the left and noble-fir branch samples are shown on the right.

so it is cheaper to produce. Plywood requires thin, long sheets of wood veneers. Similar trends have been seen in other countries, including Japan (see Fig. 4).

As part of this study, a radiant heat flux of 25–30 kW/m<sup>2</sup> was applied and the spark was operated continuously to produce flaming combustion. Under these conditions, the OSB samples ignited with sustained flaming ignition within 90 s. Experiments were also conducted using a radiant heat flux of 25 kW/m<sup>2</sup>, without the application of the spark, to produce smouldering combustion.

Additional experiments were conducted by exposing natural vegetation to the exact same exposure conditions as were done for the structural fuels. Samples of noble-fir branches were taken from tree specimens and prepared for exposure to radiant heat. Specifically, the branches were cut into pieces of 50 mm in length. These were then oven dried at 104°C for 16 h. The branches consisted of conifer needles as well as bark and associated wood.

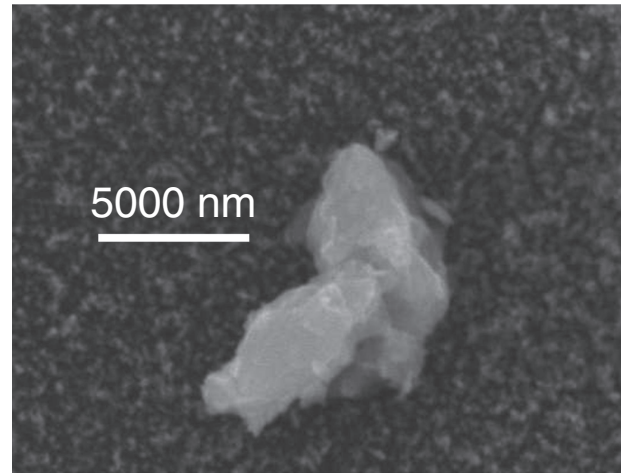


**Fig. 5.** SEM image of agglomerate with a grid insertion time of 1 s for OSB in a state of flaming combustion (30 kW/m<sup>2</sup>).

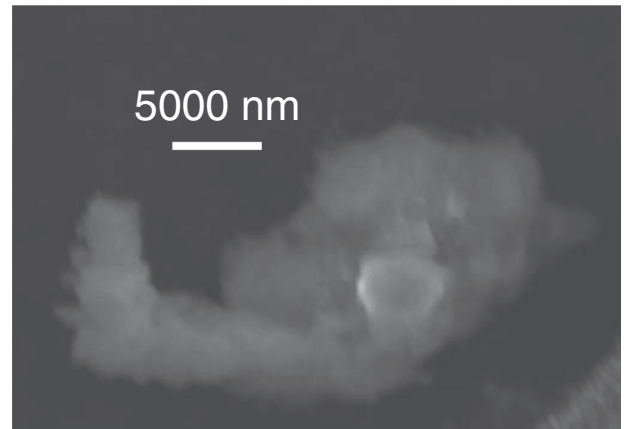


**Fig. 6.** SEM image of agglomerate with a grid insertion time of 3 s for OSB in a state of flaming combustion (25 kW/m<sup>2</sup>).

To sample particulates that are generated, the well-known principle of thermophoretic sampling was used. In the presence of a temperature gradient, the hot particles will be collected using cold grids (Oken Shoji #10-1012) that may be used for Scanning Electron Microscope (SEM) and Transmission Electron Microscopy (TEM) analysis. Here, SEM (JOEL JSM-IT500HR/LA) was used as the first step to image the overall structure of the particulate samples at 25 kV. In this study, the sampling time used was varied from 1 to 2 s, up to 3 s. Namely, the grid was inserted in the flame for these times.

## Results and discussion

Experiments were conducted for one applied heat flux level and all samples were taken at the same time after the onset of sustained flaming combustion of the OSB sample. The total sampling time varied from 1 to 3 s. Figs 5, 6 display

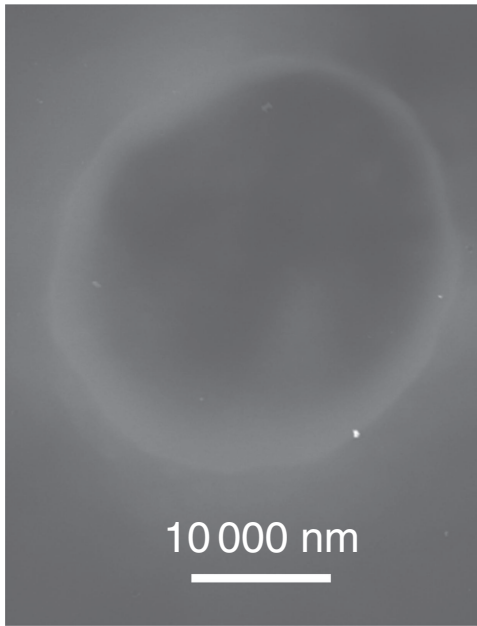


**Fig. 7.** SEM image of liquid-like particles collected from OSB in a state of smouldering combustion ( $25 \text{ kW/m}^2$ ).

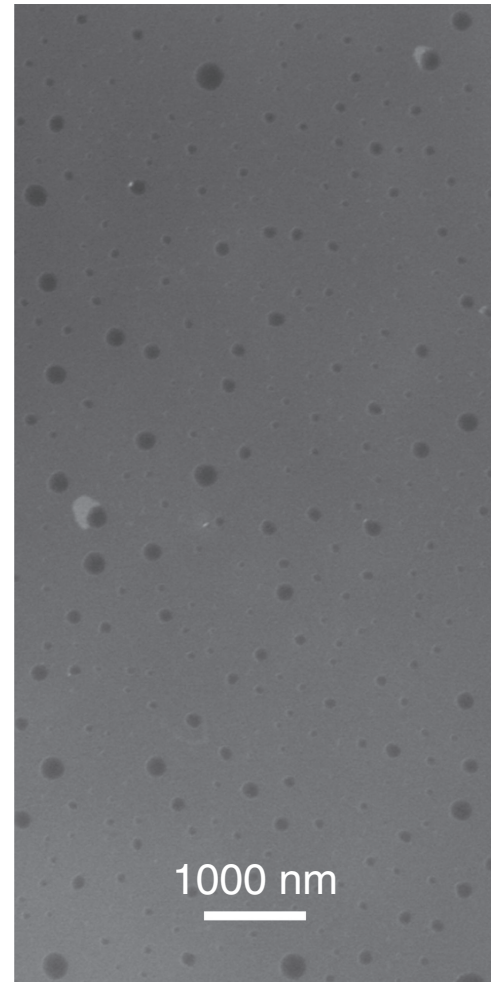


**Fig. 9.** SEM image of liquid-like particles collected from OSB in a state of smouldering combustion ( $25 \text{ kW/m}^2$ ).

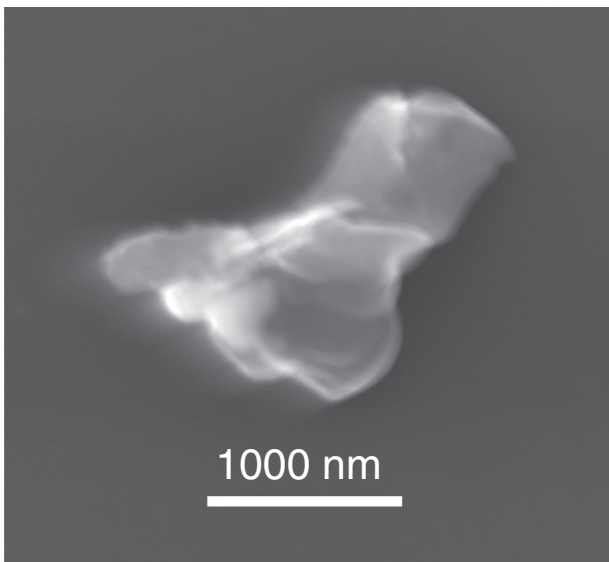


**Fig. 8.** SEM image of particulate samples collected from OSB in a state of smouldering combustion ( $25 \text{ kW/m}^2$ ).

agglomerates imaged with the SEM for two different sampling times. It is interesting to observe that the structure of the agglomerates is not markedly different between the two sampling times.

A series of experiments were conducted to sample the particulates generated from OSB samples in a state of smouldering combustion. The radiant heat flux was applied to the specimens and no spark was applied. Typical SEM images for the collected particulates from OSB undergoing smouldering combustion are displayed in Figs 7–9.

The morphology of the particulates is indeed different depending on whether the OSB samples are in a state of flaming as opposed to smouldering combustion. Owing to the higher temperatures during flaming combustion, the more well-known fractal agglomerate structures are observed for the OSB samples in a state of flaming combustion.

To provide a direct comparison, particulates were collected from vegetative samples. Noble-fir was used as a surrogate for various wildland fuels that may be present. The vegetative samples were exposed to a radiant heat flux of  $25 \text{ kW/m}^2$  and, since smouldering combustion was desired, no spark was applied. The particulate samples were collected using the sampling system described above. The insertion time of the sampling probe was varied to observe any differences in the particulates that were collected. Since particulate samples were very interesting for the structural fuels during the smouldering combustion phase, it was desired to compare these directly to vegetative fuels.

Fig. 10 displays a typical particulate sample collected in the smouldering combustion phase. This sample was collected

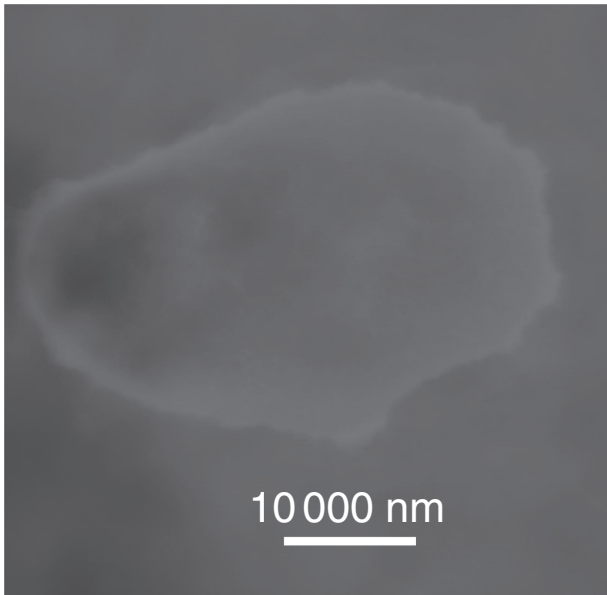


**Fig. 10.** Particulate sample collected during the smouldering combustion phase from noble-fir branches exposed to a radiant heat flux of  $25 \text{ kW/m}^2$ .

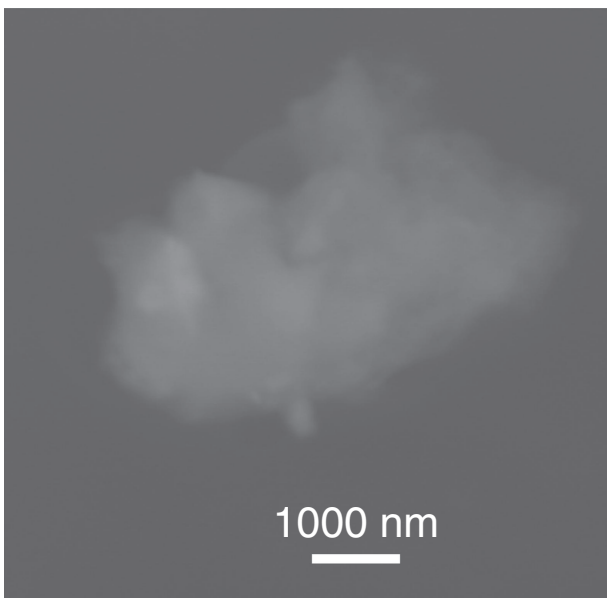


**Fig. 11.** SEM image of particulate samples collected from noble-fir branches in a state of smouldering combustion.

30 s after the onset of smouldering combustion. Similar to the particulate samples collected for structural fuels, the particulates appear liquid-like in structure. It is clear to see that the sizes of the liquid particles appear larger than those collected for the structural fuels under similar conditions.

Fig. 11 displays another particulate sample collected under the same smouldering combustion conditions. In addition to the large liquid-like samples collected, there are also several smaller-sized particulate samples collected under the

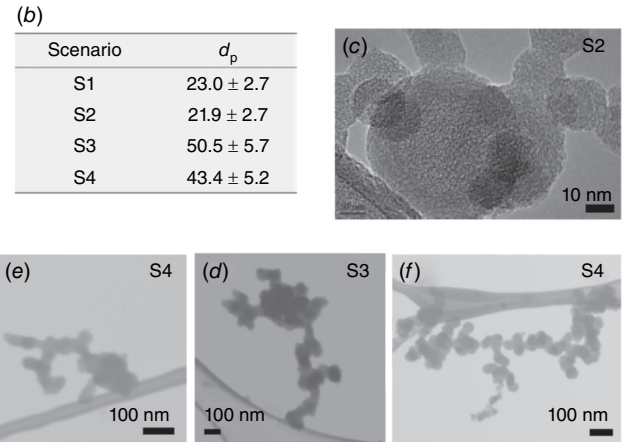


**Fig. 12.** Images collected by Okyay *et al.* (2018) for particulate samples collected using thermophoretic sampling for balsa composite specimens in flaming combustion.

same smouldering conditions that appear to be slightly more carbonaceous in form.

While the SEM images are useful, TEM analysis is helpful to provide finer details of the interior structures of the particles and is also better suited to applying image analysis methods to determine important physical characteristics (Manzello and Choi 2002). These differences are due to the scanning as opposed to transmission electron microscopy techniques. Yet, SEM generally operates at lower electron beam voltages, and it is expected that the liquid-like particles are very sensitive to these parameters, so SEM was used as the first step.

Detailed comparisons were undertaken for particulate samples collected from structural fuel sources. In the investigation by Okyay *et al.* (2018), particulate samples were collected from balsa composite specimens during flaming combustion. Specifically, the balsa samples were exposed to radiant heat fluxes ranging from  $35$  to  $50 \text{ kW/m}^2$ , ignited with a spark ignition source, and particulate samples were collected during flaming combustion using thermophoretic sampling. The balsa sample size used for particulate sample collection was identical to those used here ( $100 \text{ mm} \times 100 \text{ mm}$ ). The specifics of the balsa samples contained both the balsa core and a composite core with layers made of glass fibres inserted into a polyester resin. In this work, the particulate samples were imaged using a combination of SEM and TEM. Overall, the particulate samples exhibited properties typical of carbonaceous soot agglomerates. Namely fractal chain agglomerates comprised of nearly spherical individual primary particles. For a direct comparison of the structures observed in the present work, Fig. 12 is provided.

Additional work that has been conducted to investigate particulate morphology from simulated large fires is work that has been conducted for large-scale pool fires. Although the fuel sources are liquid fuels, it is of interest to compare these findings since large-scale pool fires are believed to be a

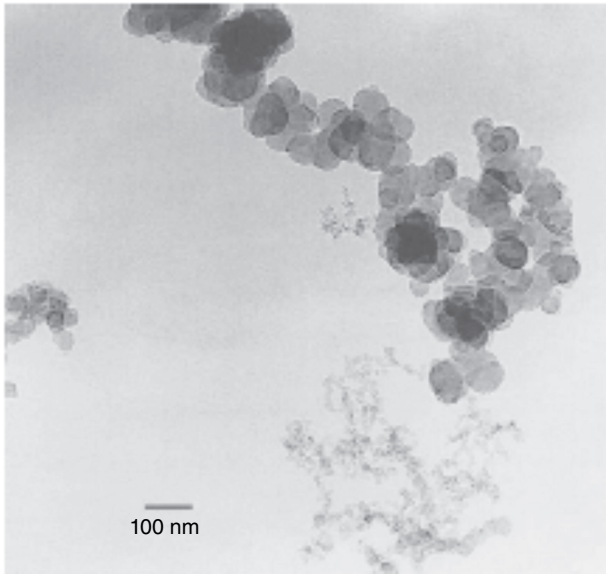
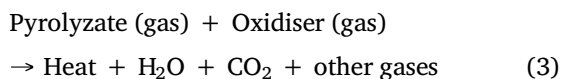
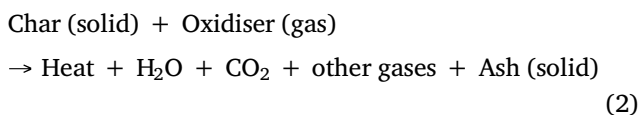
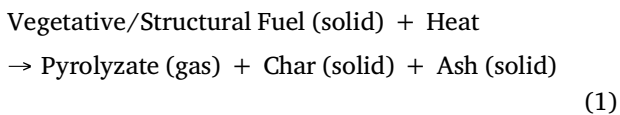


**Fig. 13.** Images from JP-8 5.0 m pool fires showing the morphology of the collected particulates (Williams and Gritzo 1998).

surrogate for large outdoor fires in general. Williams and Gritzo (1998) compared particulate morphology from JP-8 pool fires of 5.0 m in diameter to the morphology collected from laminar ethylene diffusion flames. In these interesting studies, high-resolution TEM (HRTEM) was undertaken. Fig. 13 displays the collected particulate morphology from the JP-8 pool fires. Once again, well known fractal structures, typically seen for soot agglomerates were observed.

Perhaps the most interesting finding of the present work is that the particulate samples collected from the smouldering combustion phase using thermophoretic sampling are quite different in their morphology as compared to flaming combustion. Fractal agglomerate structures were not observed and the particulates did indeed appear liquid-like in their composition.

To understand these differences, it is useful to consider the basics of smouldering combustion as opposed to flaming combustion. The following reactions are considered (Manzello and Suzuki 2022):



While the pyrolysis reaction (Eqn 1), is necessary for both smouldering and flaming combustion, flaming combustion,

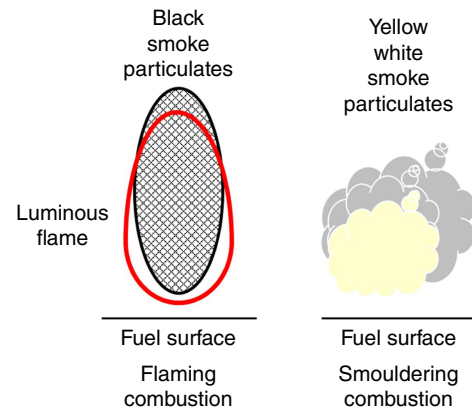


**Fig. 14.** Drawings showing differences in particulates observed during flaming combustion and smouldering combustion states.

namely reaction (Eqn 3), yields much higher temperatures in the luminous flame zone. As such, when sampling particulates from the OSB and noble-fire samples in a state of flaming combustion, it is expected to see agglomerates with a fractal structure.

Smouldering combustion is much more complex. Polyaromatic species from the surface continue to decompose in the gas-phase and then cool sufficiently to condense and form aerosol particles (Reid *et al.* 2005). In the case of flaming combustion conditions, these same polyaromatic species further decompose and the concentrations of the decomposed materials are such that they are not fully consumed in the flame and are emitted as soot particles. For smouldering combustion conditions, larger size aerosols may be expected if the condensation and growth on nucleation sites are present where the large carbon number PAH are coming from the surface into the cold gases. Therefore, the liquid-like particles just continue to grow in a lower temperature regime. These processes are illustrated in Fig. 14.

Lastly, the particle sizes were analysed for the OSB particulates collected in a state of smouldering combustion. Multiple SEM images were collected for a sampling time of 60 s after the onset of smouldering combustion. The total insertion time of the sampling probe was 1 s. Since most of the liquid-like particles are nearly spherical, the diameters of these were measured and are reported in Fig. 15. As a direct comparison, Fig. 16 displays the results of the particle size analysis for the noble-fir particulates collected in state of smouldering combustion under identical sampling conditions.

To determine the particle diameters, commercial image processing software was used. The uncertainty in determining the particle diameters comes from properly identifying the edges of the particles from the background and the inherent uncertainty in the reported magnification reported by the SEM itself. Based on two factors, the uncertainty in the reported particle diameter is  $\pm 5\%$ .

As may be seen, very small liquid-like particulates dominate the distribution but it is interesting to observe some

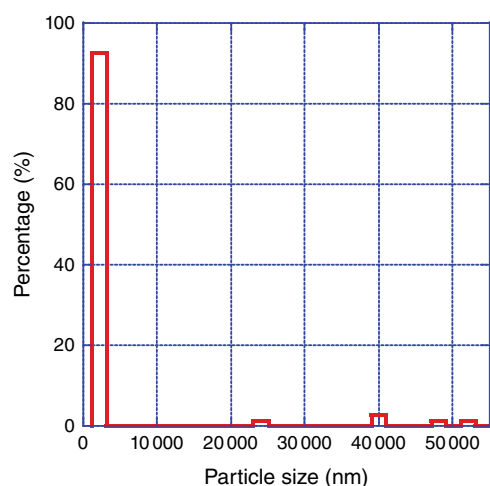


**Fig. 15.** Analysis of liquid particle sizes sampled from smouldering combustion of OSB samples. The grid insertion time was 1 s and the samples were taken 60 s after the onset of smouldering combustion. The uncertainty in determining the particle diameter was  $\pm 5\%$ . A total of 75 particles were analysed.

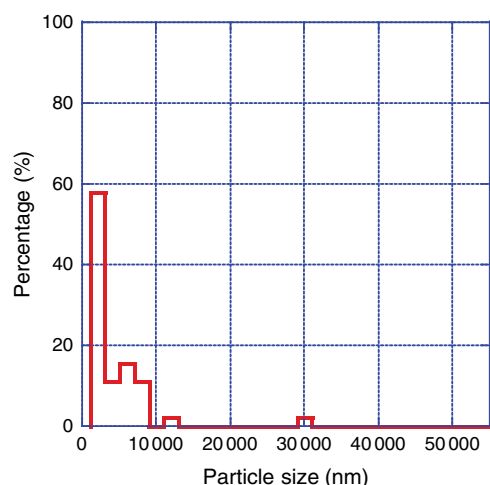


**Fig. 16.** Analysis of liquid particle sizes sampled from smouldering combustion of noble-fir branches. The grid insertion time was 1 s and the samples were taken 60 s after the onset of smouldering combustion. The uncertainty in determining the particle diameter was  $\pm 5\%$ . A total of 45 particles were analysed.

very large particles present as well, mainly for the OSB particulates. More than 85% of the analysed particle diameters were less than 1000 nm in size for the OSB particulates. In the case of noble-fir particulates, 47% of the analysed particle diameters were less than 1000 nm. Irrespective of the two fuels considered, under smouldering combustion conditions, there is a plethora of small particles generated.

Finally, an important aspect to consider is the production of ash from the combustion processes. With regards to ash, there is an excellent review on this topic published recently by Kleinhans *et al.* (2018) as well as an international team

from a wildland fire point of view (Bodí *et al.* 2014). From both reviews, it is apparent the particles in this study are not ash. The morphologies do not look even remotely close to ash particles and temperatures are too high at the collection point to be ash.

## Summary

Particulate samples were taken during both flaming combustion states and smouldering combustion states using thermophoretic sampling. As a direct comparison to the results from the engineered cellulosic-based material experiments, branches from noble-fir trees were also exposed to a radiant heater and particulate samples were collected using similar experimental protocols. The nature of the combustion state, that is smouldering combustion as opposed to flaming combustion, resulted in vast differences in the morphology of the collected samples. A detailed analysis was undertaken for the liquid-like particles that were collected using SEM and subsequent image processing. More than 85% of the analysed particle diameters were less than 1000 nm in size for the OSB particulates during smouldering combustion. In the case of noble-fir particulates, 47% of the analysed particle diameters were less than 1000 nm during smouldering combustion.

The findings of the present study are only a first step to better quantify the morphology of particulates generated during large outdoor fire outbreaks. For example, OSB is not the only engineered cellulosic material found in the built environment but there are many others in common use, including plywood and various cross-laminated timbers (CLT). Furthermore, there are a plethora of polymeric-based materials as well that combusted during large outdoor fires.

While the SEM images are useful, TEM analysis, and in particular high-resolution TEM (HRTEM) is needed to provide finer details of the interior structures of the particulates. A challenge is the higher operating voltages present in most TEM systems, especially those present in high resolution applications. It is hoped to explore these measurements in the future.

## References

- Akagi SK, Yokelson RJ, Wiedinmeyer C, *et al.* (2011) Emission Factors for Open and Domestic Biomass Burning for Use in Atmospheric Models. *Atmospheric Chemistry and Physics* **11**, 4039–4072. doi:10.5194/acp-11-4039-2011
- Bento-Gonçalves A, Vieira A (2020) Wildfires in the wildland-urban interface: key concepts and evaluation methodologies. *Science of The Total Environment* **707**, 135592. doi:10.1016/j.scitotenv.2019.135592
- Bodí MB, Martin DA, Balfour VN, *et al.* (2014) Wildland fire ash: Production, composition and eco-hydro-geomorphic effects. *Earth-Science Reviews* **130**, 103–127. doi:10.1016/j.earscirev.2013.12.007
- Chas-Amil ML, Touza J, García-Martínez E (2013) Forest fires in the wildland–urban interface: A spatial analysis of forest fragmentation and human impacts. *Applied Geography* **43**, 127–137. doi:10.1016/j.apgeog.2013.06.010
- Chen HX, Dobbins RA (2000) Crystallogensis of particles formed in hydrocarbon combustion. *Combustion Science and Technology* **159**, 109–128. doi:10.1080/00102200008935779

- Das Chowdhury K, Howard JB, Vander Sande JB (1996) Fullerene nanostructures in flames. *Journal of Materials Research* **11**, 341–347. doi:10.1557/JMR.1996.0040
- Dobbins RA (1997) The early soot particle formation in hydrocarbon flames. In 'Physical and Chemical Aspects of Combustion: A Tribute to Irvin Glassman'. (Eds FL Dryer, RF Sawyer) pp. 107–133. (Gordon and Breach Science Publishers: The Netherlands)
- Dobbins RA (2007) Hydrocarbon Nanoparticles Formed in Flames and Diesel Engines. *Aerosol Science and Technology* **41**, 485–496. doi:10.1080/02786820701225820
- Dobbins RA, Megaridis CM (1987) Morphology of Flame-Generated Soot as Determined by Thermophoretic Sampling. *Langmuir* **3**, 254–259. doi:10.1021/la00074a019
- Grieco WJ, Howard JB, Rainey LC, Vander Sande JB (2000) Fullerene carbon in combustion-generated soot. *Carbon* **38**, 597–614. doi:10.1016/S0008-6223(99)00149-9
- Hebgen P, Goel A, Howard JB, Rainey LC, Vander Sande JB (2000) Synthesis of fullerenes and fullerene nanostructures in a low-pressure benzene/oxygen diffusion flame. *Proceedings of the Combustion Institute* **28**, 1397–1404. doi:10.1016/S0082-0784(00)80355-0
- Hemes KS, Verfaillie J, Baldocchi DD (2020) Wildfire-Smoke Aerosols Lead to Increased Light Use Efficiency Among Agricultural and Restored Wetland Land Uses in California's Central Valley. *Journal of Geophysical Research: Biogeosciences* **125**, e2019JG005380. doi:10.1029/2019JG005380
- Hu Y, Fernandez-Anez N, Smith TEL, Rein G (2018) Review of emissions from smouldering peat fires and their contribution to regional haze episodes. *International Journal of Wildland Fire* **27**, 293–312. doi:10.1071/WF17084
- Kleinhans U, Wieland C, Frandsen FJ, et al. (2018) Ash formation and deposition in coal and biomass fired combustion systems: Progress and challenges in the field of ash particle sticking and rebound behavior. *Progress in Energy and Combustion Science* **68**, 65–168. doi:10.1016/j.peccs.2018.02.001
- Lighty JS, Veranth JM, Sarofim AF (2000) Combustion Aerosols: Factors Governing Their Size and Composition and Implications to Human Health. *Journal of the Air & Waste Management Association* **50**, 1565–1618. doi:10.1080/10473289.2000.10464197
- Manzello SL, Choi MY (2002) Morphology of Soot Collected in Microgravity Droplet Flames. *International Journal of Heat and Mass Transfer* **45**, 1109–1116. doi:10.1016/S0017-9310(01)00164-8
- Manzello SL, Suzuki S (2022) The Importance of Combustion Science to Unravel Complex Processes for Informal Settlement Fires, Urban Fires, and Wildland-Urban Interface (WUI) Fires. *Fuel* **314**, 122805. doi:10.1016/j.fuel.2021.122805
- Michelsen HA (2017) Probing Soot Formation, Chemical and Physical Evolution, and Oxidation: A Review of *in situ* diagnostic Techniques and Needs. *Proceedings of the Combustion Institute* **36**, 717–735. doi:10.1016/j.proci.2016.08.027
- Okay G, Bellayer S, Samyn F, Jimenez M, Bourbigot S (2018) Characterization of In-Flame Soot from Balsa Composite Combustion during Mass Loss Cone Calorimeter Tests. *Polymer Degradation and Stability* **154**, 304–311. doi:10.1016/j.polymdegradstab.2018.06.013
- Pósfai M, Simonics R, Li J, Hobbs PV, Buseck PR (2003) Individual Aerosol Particles from Biomass Burning in Southern Africa: 1. Compositions and Size Distributions of Carbonaceous Particles. *Journal of Geophysical Research: Atmospheres* **108**, 8483. doi:10.1029/2002JD002291
- Reid JS, Koppmann R, Eck TF, Eleuterio DP (2005) A Review of Biomass Burning Emissions Part II: Intensive Physical Properties of Biomass Burning Particles. *Atmospheric Chemistry and Physics* **5**, 799–825. doi:10.5194/acp-5-799-2005
- Reisen F, Duran SM, Flannigan M, et al. (2015) Wildfire Smoke and Public Health Risk. *International Journal of Wildland Fire* **24**, 1029–1044. doi:10.1071/WF15034
- Shaddix CR, Palotás ÁB, Megaridis CM, Choi MY, Yang NYC (2005) Soot graphitic order in laminar diffusion flames and a large-scale JP-8 pool fire. *International Journal of Heat and Mass Transfer* **48**, 3604–3614. doi:10.1016/j.ijheatmasstransfer.2005.03.006
- Suzuki S, Manzello SL (2021) Investigating Coupled Effect of Radiative Heat Flux and Firebrand Showers on Ignition of Fuel Beds. *Fire Technology* **57**, 683–697. doi:10.1007/s10694-020-01018-5
- Vander Wal RL, Tomasek AJ (2003) Soot oxidation: dependence upon initial nanostructure. *Combustion and Flame* **134**, 1–9. doi:10.1016/S0010-2180(03)00084-1
- Wang H (2011) Formation of Nascent Soot and Other Condensed Phase Materials in Flames. *Proceedings of the Combustion Institute* **33**, 41–67. doi:10.1016/j.proci.2010.09.009
- White RS, Winandy G (2006) Fire Performance of Oriented Strand Board (OSB). In 'Proceedings of the Conference on Recent Advances in Flame Retardancy of Polymeric Materials: volume XVII, Applications, Research and Industrial Development Markets'. pp. 297–390. (BCC: Norwalk, CT)
- Williams JM, Gritz LA (1998) *in situ* Sampling and Transmission Electron Microscope Analysis of Soot in the Flame Zone of Large Pool Fires. *Symposium (International) on Combustion* **27**, 2707–2714. doi:10.1016/S0082-0784(98)80126-4

**Data availability.** The data presented in this manuscript is available from the authors upon reasonable request.

**Conflicts of interest.** The authors declare no conflict of interest.

**Declaration of funding.** This research did not receive any specific funding.

#### Author affiliations

<sup>A</sup>National Research Institute of Fire and Disaster (NRIFD), Chofu, Tokyo, Japan.

<sup>B</sup>Reax Engineering, Berkeley, CA, USA.